

Kinetic Modeling for Vesicle Drug Delivery to the Liver

Michael Liao
CJ Norsigian
Michael Salazar

BENG 221
October 5, 2016

Contents

Introduction	3
Hepatic Receptor Study	4
Problem Statement	5
Methods	5
Analytical Solution of Simplified Model	7
Complex Model and Numerical Analysis	10
Parameter Values	13
Conclusion	14
References	16
Appendix of Code	17

Introduction

Vesicles have long been shown to be useful drug carriers in a variety of situations. Drug delivery by these means have the advantages of protecting drugs from degradation, increasing the half-life in the blood stream, and targeted delivery. Liver disease is one area in which vesicle drug delivery has been shown to have potential as an effective therapy. There are over 100 different types of liver disease ranging from mild to severe that affect all ages and 30 million Americans alone. There is a plethora of drugs that can be loaded into vesicles to slow the progression of these debilitating diseases. The benefits of this delivery system are substantial in liver diseases, such as liver cancer and hepatitis, for which available drugs exhibit significant extrahepatic toxicity, low hepatic clearance rates, and/or are rapidly metabolized before reaching their site of action.

Currently, one method of drug delivery to the liver is through the parenteral route of administration, and more specifically, intravenous injection. This route is the fastest and most controlled method to deliver drugs to systemic circulation, bypassing first pass metabolism and the gastro intestinal tract. This method is commonly used when continuous or large volumes of drugs need to be administered. Additionally, intravenous delivery methods can result in faster systemic absorption resulting in faster therapeutic effect, however also increases the potential for harmful off target side-effects. For this reason, encapsulation of drug compounds within vesicles may limit off target exposure and reduce the chance of negative side effects common in

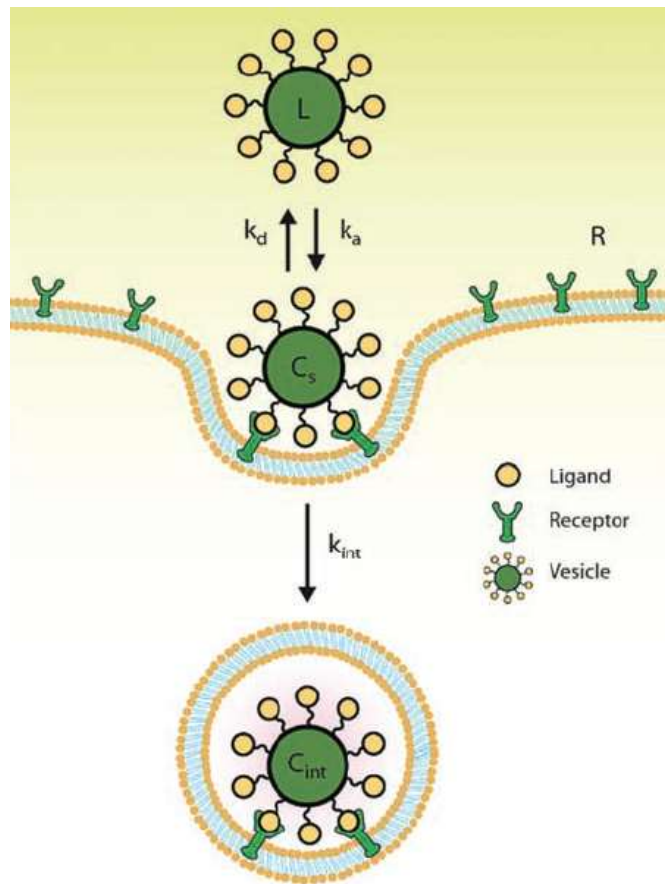


Figure 1: Simple schematic showing the process of a vesicle with target ligands binding to the cell wall and being endocytosed.

intravenously administered therapeutics. Upon reaching the targeted region within the liver, interactions between a specific vesicle conjugated ligand and cell surface receptor mediate either the fusion of the vesicle with the cellular membrane, or endocytosis of the vesicle, releasing the therapeutic compound in a controlled process to the local area.

Applying mathematical modeling to the kinetics of vesicle drug delivery can better inform treatment schemes as well as reduce the time and resources needed to make these therapies a reality. In this investigation we explore the use of the asialoglycoprotein receptor in particular due to its established physiological properties within the target tissue of the liver. However, the general structure of the models can apply to many different specific receptors if the relevant constants are updated. Target ligands conjugated to the surface of vesicles allow the vesicles to be endocytosed by cells via natural mechanisms. It is worth noting that receptor and ligand interactions are not permanent and dissociation of the vesicle can occur. Mass-action kinetics are a useful method to model the cellular uptake of these vesicles. In biology there can be more than one ligand-receptor interaction per vesicle. This multivalency while biologically relevant can be simplified for modeling purposes to consider the sum of these interactions in terms of a 1:1 ratio for vesicle-binding site interactions. Mathematical models built on reaction kinetics can be used to evaluate the rate of internalization of vesicles into targeted cells.

Hepatic Receptor Study^[1]

Liver perfusions were performed in the previous literature to analyze the efficacy of liver targeted vesicles and their interactions with hepatic parenchymal cells in treating liver disease¹. The single bilayer vesicles were primarily composed of cholesterol, DPPC and DGDG and loaded with ¹⁴[C]sucrose or ¹⁴[C]carboxyinulin to measure vesicle binding and biodistribution. Intravenous injections were performed in the tails of 15 adult male Spague-Dawley rats.

This previous study incorporated the in vivo results obtained to develop a pharmacokinetic model of vesicle disposition, which can be used to predict vesicle clearance, internalization, and concentration in blood^[1]. We analyzed the model presented in Dragsten, et al. in its full form as well as a more simplified case.

Problem Statement

In this project we examined two models for the uptake of vesicles by the liver: one simple model to study analytically and one more complex model to study utilizing numerical methods. This involves three separate processes, the transportation of the vesicles to the liver, binding, uptake and regeneration of receptors. We analyzed the effect of varying rate constants on the eventual cellular uptake of vesicles by the target cell and demonstrate the change in receptor-vesicle states over time.

Methods

A relevant approach to model vesicle-receptor interaction in drug delivery is mass action kinetics. The central principle of mass action kinetics is that the change in rate of a given reaction is linearly proportional via some rate constant to the current mass. In the case of vesicle drug delivery both the vesicles and receptors can be modeled this way where reactions here represent the changing state of both of these entities. To describe vesicle drug delivery utilizing mass action kinetics the following assumptions were made:

1. We simplify the amount of ligand-receptor interactions that can occur per vesicle. It is easier to disregard multivalency for modeling purposes and consider the sum of these interactions as a 1:1 ratio
2. We also assume that the regeneration of receptors occurs at a balanced rate that corresponds to the changes in free and bound receptors. This may not be how cells exactly replenish receptors in a biological setting. This assumption is intrinsic to the loop from I back to R in our network diagram.
3. The effects of heat, diffusion, and transport time in space are not explicitly considered, these would introduce complex partial differential equations into the model.

The first model we propose (See Figure 2) demonstrates the balance of receptor-vesicle complexes with the key assumption that vesicles are infinitely plentiful. This assumption will be changed in the second more complex model.

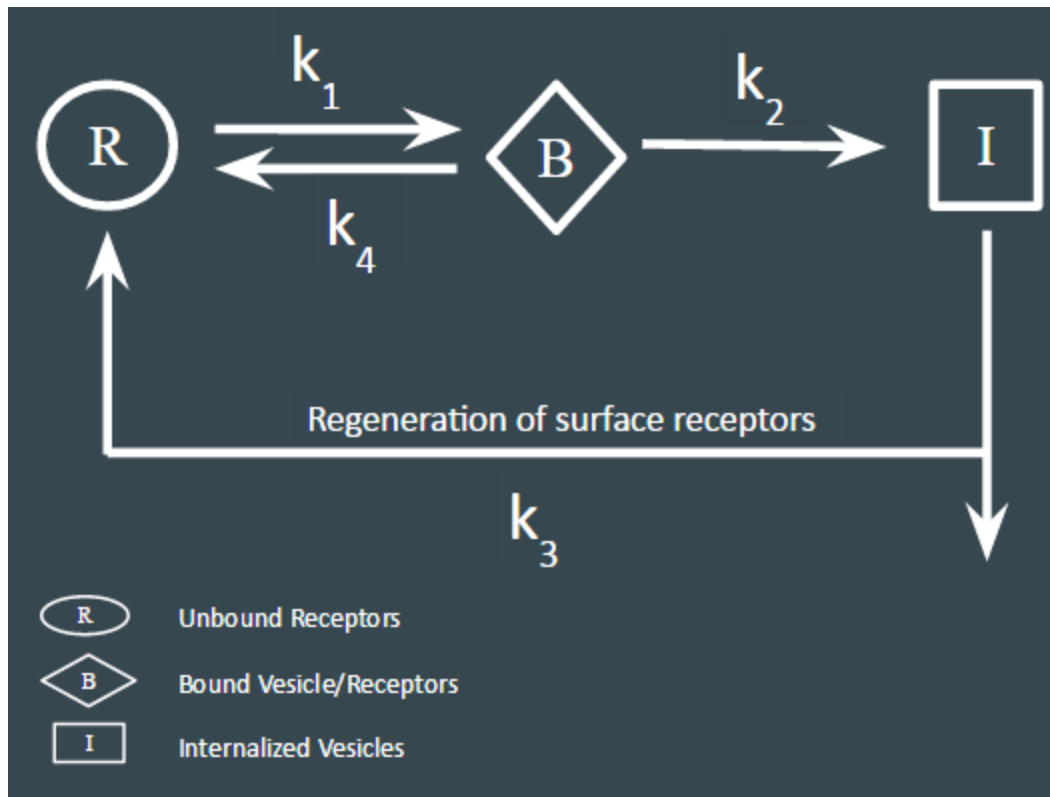


Figure 2: Network representation of the simplified model depicting the flow of vesicle-receptor complexes.

R in this network represents the concentration of unbound receptors, B represents the concentration of receptor-vesicle bound complexes, and I represents the concentration of vesicles that have been internalized into the cell. R depends on the rate constant, k_1 , for receptors going to the bound state as ligand-receptor binding occurs. Complexes in the B state also can revert back to the R state when vesicles dissociate from the receptors via the rate constant k_4 . R is finally also affected proportionally by the rate, k_3 , which represents the transition from I to R meaning biologically that new cell receptors are being presented on the surface after the endocytosis. B depends on both its forward and backward state changes with R as well as the forward change from a bound receptor-complex to the I state proportional to the rate constant k_2 .

This model network of vesicle-receptor behavior can also be represented by the following set of ordinary differential equations via the principles of mass action kinetics:

$$\frac{dR}{dt} = k_3I - k_1R + k_4B$$

$$\frac{dB}{dt} = k_1R - k_2B - k_4B$$

$$\frac{dI}{dt} = k_2B - k_3I$$

There is utility in going through the analytical solution for this system before using numerical methods on a more complex model that involves the movement of injected vesicles in and out of target tissue.

Analytical Solution of Simplified Model

The system of linear differential equations can be written in matrix form to facilitate solving for the eigenvalues and vectors. The first step in this process involves crafting the following coefficients matrix for the above system of ordinary differential equations:

$$\begin{vmatrix} k_1 - \lambda & k_4 & k_3 \\ k_1 & (-k_2 - k_4) - \lambda & 0 \\ 0 & k_2 & -k_3 - \lambda \end{vmatrix}$$

The eigenvalues (λ) and corresponding vectors (v) are shown below. From these values the general solution can be formed. The general solution obtained from these eigenvalues and vectors allows for a solution of the constants by plugging in the initial conditions and parameter values (See Table 1).

$$\lambda_1 = 0$$

$$\lambda_2 = -\frac{1}{2}\sqrt{(k_1 + k_2 + k_3 + k_4)^2 - 4(k_1k_2 + k_1k_3 + k_2k_3 + k_3k_4)} - k_2 - k_3 - k_1 - k_4$$

$$\lambda_3 = \frac{1}{2} \sqrt{(k_1 + k_2 + k_3 + k_4)^2 - 4(k_1k_2 + k_1k_3 + k_2k_3 + k_3k_4)} - k_2 - k_3 - k_1 - k_4$$

$$v_1 = \begin{pmatrix} \frac{k_3(k_2 + k_4)}{k_1k_2} \\ \frac{k_3}{k_2} \\ 1 \end{pmatrix}$$

v_2

$$= \begin{pmatrix} \frac{1}{4k_1k_2} \left(k_1 - k_2 + k_3 - k_4 + \sqrt{(k_1 + k_2 + k_3 + k_4)^2 - 4(k_1k_2 + k_1k_3 + k_2k_3 + k_3k_4)} \right) \dots \\ \dots * \left(k_1 + k_2 - k_3 + k_4 + \sqrt{(k_1 + k_2 + k_3 + k_4)^2 - 4(k_1k_2 + k_1k_3 + k_2k_3 + k_3k_4)} \right) \\ -k_3 + \frac{1}{2} \left(k_1 + k_2 + k_3 + k_4 + \sqrt{(k_1 + k_2 + k_3 + k_4)^2 - 4(k_1k_2 + k_1k_3 + k_2k_3 + k_3k_4)} \right) \\ \hline \frac{k_2}{1} \end{pmatrix}$$

v_3

$$= \begin{pmatrix} \frac{1}{4k_1k_2} \left(k_1 - k_2 + k_3 - k_4 - \sqrt{(k_1 + k_2 + k_3 + k_4)^2 - 4(k_1k_2 + k_1k_3 + k_2k_3 + k_3k_4)} \right) \dots \\ \dots * \left(k_1 + k_2 - k_3 + k_4 - \sqrt{(k_1 + k_2 + k_3 + k_4)^2 - 4(k_1k_2 + k_1k_3 + k_2k_3 + k_3k_4)} \right) \\ -k_3 + \frac{1}{2} \left(k_1 + k_2 + k_3 + k_4 - \sqrt{(k_1 + k_2 + k_3 + k_4)^2 - 4(k_1k_2 + k_1k_3 + k_2k_3 + k_3k_4)} \right) \\ \hline \frac{k_2}{1} \end{pmatrix}$$

The steady-state solutions of this system are easily calculated by setting the rates of change of each state to zero and are as follows:

$$R = \frac{k_3I + k_4B}{k_1}$$

$$B = \frac{k_1R}{k_2 + k_4}$$

$$I = \frac{k_2B}{k_3}$$

Graphing the solution to this system demonstrates the biological relevance of the model solution (See Figure 3). As would be expected the values of R decrease over the specified time period as the B and I states both increase, however with B increasing more rapidly at first then allowing I to also increase. These trends make logical sense when remembering the biological scenario being modeled as unbound receptors decrease with corresponding increase in bound receptor-vesicle complexes, followed by an increase in the internalization of those receptor-vesicle complexes.

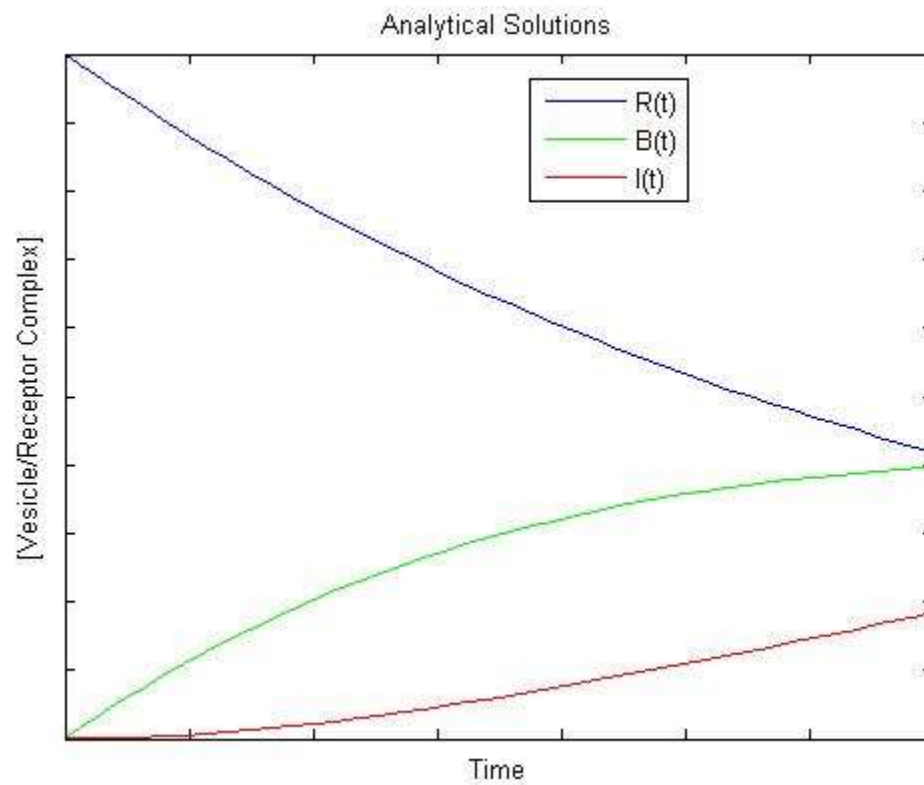


Figure 3: Solution of the simplified model plotted. These results align with the biological relevance as R is shown to decrease while B and I both increase at appropriate rates.

Complex Model and Numerical Analysis

As previously noted a critical assumption made to simplify the first model was that vesicles were not a limiting factor, here we introduce representation for the spatial difference in vesicle concentration as outlined in Dragsten et al. We now introduce C_1 , C_2 , k_{qb} , and k_{qa} to include the balance of vesicles reaching the target liver tissue (See Figure 4).

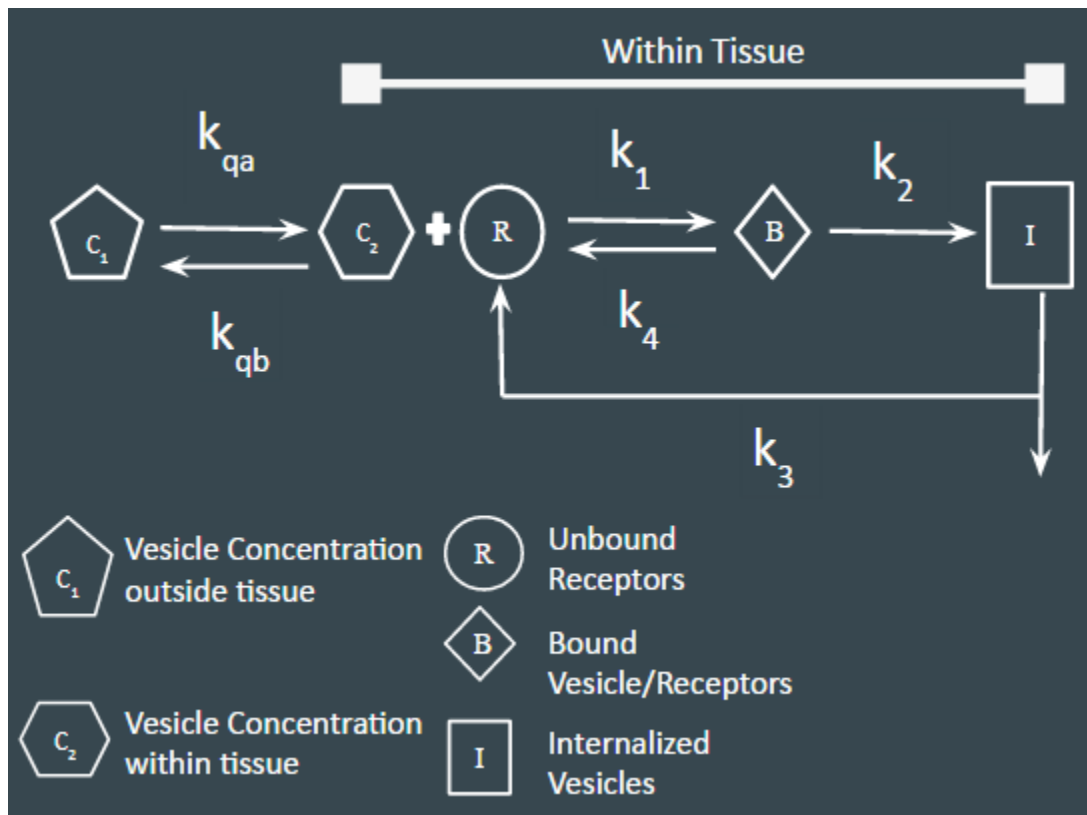


Figure 4: Complex network implementing both the simplified network as well as new terms for the concentration of vesicles.

C_1 is the concentration of vesicles outside of the tissue and C_2 is the concentration of vesicles in proximity to the receptors within the tissue and can therefore interact and engage in the receptor-vesicle balance part of the network outlined in the previous section. Here the k_{qa} and k_{qb} coefficients are representative of hepatic plasma flow rate. A key deviation from the literature we implemented was to make k_{qa} exceed k_{qb} whereas in the paper they implement a singular Q value for this flow rate. Physiologically the flow rate would not be different, but by making k_{qa} larger we incorporate that due to the targeting the receptors in C_2 should be more

prone to staying in the target tissue than reverting back to the C_1 state. This complex model with vesicle concentrations implemented can be represented by the following system of five linear differential equations.

$$\frac{dC_1}{dt} = -k_{qa}C_1 + k_{qb}C_2$$

$$\frac{dC_2}{dt} = k_{qa}C_1 - k_{qb}C_2 - k_1RC_2 + k_4B$$

$$\frac{dR}{dt} = k_3I - k_1RC_2 + k_4B$$

$$\frac{dB}{dt} = k_1RC_2 - (k_2 + k_4)B$$

$$\frac{dI}{dt} = k_2B - k_3I$$

The numerical solution of this system of five linear differential equations was obtained using ode45 in MATLAB. The behavior of the receptor-vesicle complexes mirrors what the analytical solution of the simplified model resulted in, while introducing the dependence on vesicle concentration. C_1 and C_2 compress the time scale of the receptor-vesicle behavior in the second half of the network. This intuitively makes sense as more vesicles enter the C_2 state.

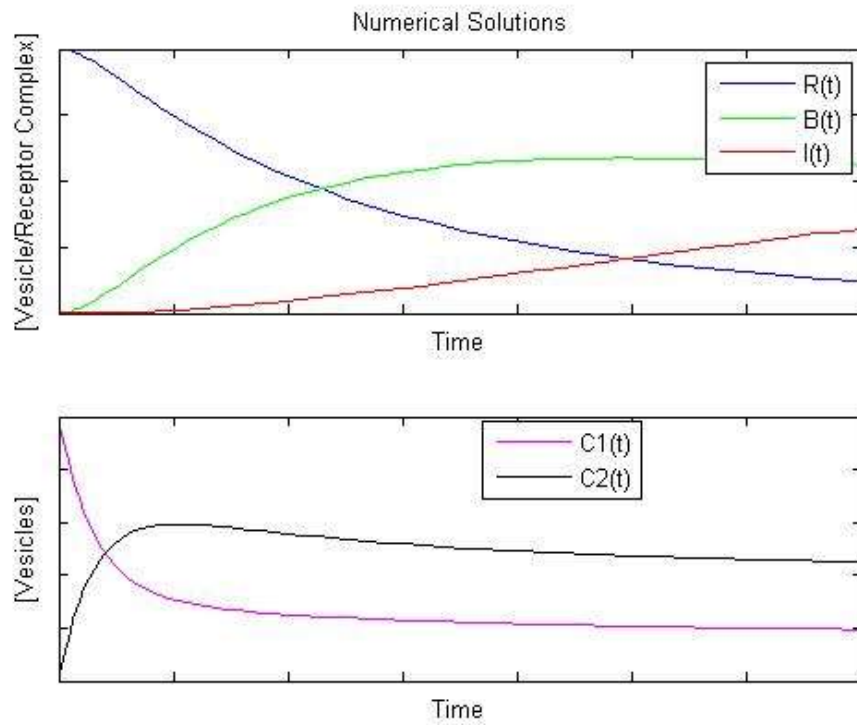


Figure 5: Solution of the complex model plotted. The essential behavior of R , B , and I is maintained from the simplified model, but a new dependence on the concentration of vesicles accelerates this behavior.

Parameter Values

Parameter values of reasonable physiological scale as reported in the literature (CITE) are shown in Table 1 below. These are the values used throughout our models and simulations.

Table 1: Parameter and Initial Condition values used for the model

Parameter	Description	Value	Units
k_1	Rate constant for unbound receptors transitioning to bound	0.128	mL/ μ g/min
k_2	Rate constant for bound vesicle-receptors being internalized	0.102	min ⁻¹
k_3	Rate constant for regeneration of unbound receptors from the internalization	0.0102	NA
k_4	Rate constant for bound vesicle-receptor complex dissociating back to unbound	0.0048	min ⁻¹
k_{qa}	Value representing the hepatic flow of vesicles into the liver tissue	2.275	ml/min
k_{qb}	Value representing the hepatic flow vesicles back out of the liver tissue	0.975	ml/min
$R(0)$	The initial value at time (t=0) of unbound receptors	2	NA
$B(0)$	The initial value at time (t=0) of bound vesicle-receptors	0	NA
$I(0)$	The initial value at time (t=0) of internalized vesicle-receptors	0	NA
$C_1(0)$	The initial value at time (t=0) of vesicles outside the tissue	5	NA
$C_2(0)$	The initial value at time (t=0) of vesicles inside the tissue	0	NA

**Concentration units are relative amounts and percentages of total initial vesicle concentration.*

Conclusion and Recommendations

The interaction and uptake of vesicles by the liver was successfully modeled in two scenarios. A simplified case study was presented that demonstrated physiologically sensible results providing insights into the general behavior of the system. The more complex system previously presented by Dragsten et al. was modified then modeled to take into account the concentration of vesicles inside and outside of the liver. Introduction of these concentration terms yielded results that were similar to the analytical solution but shifted in time, suggesting that a concentration gradient as well as binding affinities speed up the interactions. Our simulation result was able to correspond to the behavior of the actual scenario we set out to model thus indicating strength of the modeling efforts. Particularly interesting is the more complex scenario where we introduce a dependence on the concentration for the concentration in and outside of the tissue. As expected the concentration within the tissue has a sharp increase relatively early in the time profile as vesicles diffuse to the target, what is interesting is that this eventually levels off with slight decrease (See Figure 5). This makes sense given how we elected to model the behavior of vesicles being bound, internalized, and critically internalized feeding to the regeneration of unbound receptors. The C2 values must drop off to accommodate this overall balance and reach steady state. Further the dynamics of the entire scenario result in an accurate portrayal of the reaction being diffusion limited, which is expected when using rate kinetics in this manner. The overall, actual mass kinetics are only dependent on the diffusion over time, which is well reflected by our simulation results.

The presented models could be improved by taking into consideration vesicle stability and loading. In order to produce a more applicable model additional interactions would also need to be taken into account. A few of these additional interactions could include the capacity of the liver to take up the vesicle, accurate modeling of vesicle trafficking through the bloodstream following IV injection, diffusion, etc.

In this project, we presented the mathematical model crafted by Dragsten et al as well as a simplified case that could be solved analytically. We also changed the constants of the model to better reflect the current capabilities of technology today. When comparing our analytical and numerical solutions it is demonstrated that both capture some of the essential behavior, but the more complex model is more biologically relevant. These types of kinetic models can be crafted

for other specific vesicle-receptor combinations and then the models can be used to improve the efficiency and efficacy of their design.

References

1. Dragsten, Paul R., et al. "Drug delivery using vesicles targeted to the hepatic asialoglycoprotein receptor." *Biochimica et Biophysica Acta (BBA)-General Subjects* 926.3 (1987): 270-279.
2. Mosley, Garrett L., Cameron D. Yamanishi, and Daniel T. Kamei. "Mathematical Modeling of Vesicle Drug Delivery Systems 1 Vesicle Formation and Stability Along with Drug Loading and Release." *Journal of laboratory automation* (2012): 2211068212457161.
3. Shikha Jain, Vikas Jain, and S. C. Mahajan, "Lipid Based Vesicular Drug Delivery Systems," *Advances in Pharmaceutics*, vol. 2014, Article ID 574673, 12 pages, 2014. doi:10.1155/2014/574673
4. Ying, Chong T., et al. "Mathematical Modeling of Vesicle Drug Delivery Systems 2 Targeted Vesicle Interactions with Cells, Tumors, and the Body." *Journal of laboratory automation* 18.1 (2013): 46-62.

Appendix of Code

```
%BENG221 Project Code
%CJ Norsigian, Michael Salazar, Michael Liao
clc
clear

%%Analytical Solution%%
syms R(t) B(t) I(t) ka kb kc kd

eqns = [diff(R,t)==kc*I-ka*R+kd*B, diff(B,t)==ka*R-kb*B-kd*B,...
        diff(I,t)==kb*B-kc*I];

cond = [R(0)==2, I(0)==0, B(0)==0];

sol = dsolve(eqns,cond);

solR(t)=sol.R;
solB(t)=sol.B;
solI(t)=sol.I; %Particular solutions to the system at question were obtained
and assigned to new variables of R, B and I below

t=[0:0.1:10];

ka= 0.128;
kb= 0.102;
kc= 0.0102;
kd= 0.0048;

t=[0:0.1:10];

R=(2*kc*(kb + kd))/(ka*kb + ka*kc + kb*kc + kc*kd) + (ka*kb*exp(-(t*(ka + kb
+ kc + kd + (ka^2 - 2*ka*kb - 2*ka*kc + 2*ka*kd + kb^2 - 2*kb*kc + 2*kb*kd +
kc^2 - 2*kc*kd + kd^2)^(1/2))))/2)*((ka/2 + kb/2 + kc/2 + kd/2 + (ka^2 -
2*ka*kb - 2*ka*kc + 2*ka*kd + kb^2 - 2*kb*kc + 2*kb*kd + kc^2 - 2*kc*kd +
kd^2)^(1/2)/2)/kb - (kb + kc)/kb)*(ka + kb + kc + kd - (ka^2 - 2*ka*kb -
2*ka*kc + 2*ka*kd + kb^2 - 2*kb*kc + 2*kb*kd + kc^2 - 2*kc*kd +
kd^2)^(1/2)))...
/ (ka*kb*(ka^2 - 2*ka*kb - 2*ka*kc + 2*ka*kd + kb^2 - 2*kb*kc + 2*kb*kd
+ ...
kc^2 - 2*kc*kd + kd^2)^(1/2) + ka*kc*(ka^2 - 2*ka*kb - 2*ka*kc + 2*ka*kd
+ kb^2 - ...
2*kb*kc + 2*kb*kd + kc^2 - 2*kc*kd + kd^2)^(1/2) + kb*kc*(ka^2 - 2*ka*kb
- 2*ka*kc + ...
2*ka*kd + kb^2 - 2*kb*kc + 2*kb*kd + kc^2 - 2*kc*kd + kd^2)^(1/2) +
kc*kd*(ka^2 - ...
2*ka*kb - 2*ka*kc + 2*ka*kd + kb^2 - 2*kb*kc + 2*kb*kd + kc^2 - 2*kc*kd +
kd^2)^(1/2)) - ...
(ka*kb*exp(-(t*(ka + kb + kc + kd - (ka^2 - 2*ka*kb - 2*ka*kc + 2*ka*kd +
kb^2 - 2*kb*kc...
+ 2*kb*kd + kc^2 - 2*kc*kd + kd^2)^(1/2))))/2)*((ka/2 + kb/2 + kc/2 + kd/2
- ...
(ka^2 - 2*ka*kb - 2*ka*kc + 2*ka*kd + kb^2 - 2*kb*kc + 2*kb*kd + ...
```

$$\begin{aligned}
& \frac{kc^2 - 2*kc*kd + kd^2)^{(1/2)}/2}{kb} - (kb + kc)/kb) * (ka + kb + kc + \dots \\
& kd + (ka^2 - 2*ka*kb - 2*ka*kc + 2*ka*kd + kb^2 - \dots \\
& 2*kb*kc + 2*kb*kd + kc^2 - 2*kc*kd + kd^2)^{(1/2)}) / (ka*kb*(ka^2 - \\
& 2*ka*kb \dots \\
& - 2*ka*kc + 2*ka*kd + kb^2 - 2*kb*kc + 2*kb*kd + kc^2 - 2*kc*kd + \\
& kd^2)^{(1/2)} \dots \\
& + ka*kc*(ka^2 - 2*ka*kb - 2*ka*kc + 2*ka*kd + kb^2 - 2*kb*kc + 2*kb*kd + \\
& kc^2 - 2*kc*kd \dots \\
& + kd^2)^{(1/2)} + kb*kc*(ka^2 - 2*ka*kb - 2*ka*kc + 2*ka*kd + kb^2 - \\
& 2*kb*kc + 2*kb*kd \dots \\
& + kc^2 - 2*kc*kd + kd^2)^{(1/2)} + kc*kd*(ka^2 - 2*ka*kb - 2*ka*kc + \\
& 2*ka*kd + \dots \\
& kb^2 - 2*kb*kc + 2*kb*kd + kc^2 - 2*kc*kd + kd^2)^{(1/2)}); \\
\\
B = & (2*ka*kc) / (ka*kb + ka*kc + kb*kc + kc*kd) - (ka*kb*exp(-(t*(ka + kb + kc + \\
& kd + \dots \\
& (ka^2 - 2*ka*kb - 2*ka*kc + 2*ka*kd + kb^2 - 2*kb*kc + 2*kb*kd + kc^2 - \\
& 2*kc*kd \dots \\
& + kd^2)^{(1/2)})) / 2) * ((ka/2 + kb/2 + kc/2 + kd/2 + (ka^2 - 2*ka*kb - \\
& 2*ka*kc + 2*ka*kd \dots \\
& + kb^2 - 2*kb*kc + 2*kb*kd + kc^2 - 2*kc*kd + kd^2)^{(1/2)} / 2) / kb - \\
& kc/kb) * (ka \dots \\
& + kb + kc + kd - (ka^2 - 2*ka*kb - 2*ka*kc + 2*ka*kd + kb^2 - 2*kb*kc + \\
& 2*kb*kd + kc^2 \dots \\
& - 2*kc*kd + kd^2)^{(1/2)})) / (ka*kb*(ka^2 - 2*ka*kb - 2*ka*kc + 2*ka*kd + kb^2 - \\
& 2*kb*kc \dots \\
& + 2*kb*kd + kc^2 - 2*kc*kd + kd^2)^{(1/2)} + ka*kc*(ka^2 - 2*ka*kb - \\
& 2*ka*kc + 2*ka*kd \dots \\
& + kb^2 - 2*kb*kc + 2*kb*kd + kc^2 - 2*kc*kd + kd^2)^{(1/2)} + kb*kc*(ka^2 - \\
& 2*ka*kb \dots \\
& - 2*ka*kc + 2*ka*kd + kb^2 - 2*kb*kc + 2*kb*kd + kc^2 - 2*kc*kd + \\
& kd^2)^{(1/2)} + kc \dots \\
& *kd*(ka^2 - 2*ka*kb - 2*ka*kc + 2*ka*kd + kb^2 - 2*kb*kc + 2*kb*kd + kc^2 \\
& - 2*kc*kd \dots \\
& + kd^2)^{(1/2)}) + (ka*kb*exp(-(t*(ka + kb + kc + kd - (ka^2 - 2*ka*kb - \\
& 2*ka*kc + 2*ka*kd \dots \\
& + kb^2 - 2*kb*kc + 2*kb*kd + kc^2 - 2*kc*kd + kd^2)^{(1/2)})) / 2) * ((ka/2 + \\
& kb/2 + kc/2 \dots \\
& + kd/2 - (ka^2 - 2*ka*kb - 2*ka*kc + 2*ka*kd + kb^2 - 2*kb*kc + 2*kb*kd + \\
& kc^2 - 2*kc*kd \dots \\
& + kd^2)^{(1/2)} / 2) / kb - kc/kb) * (ka + kb + kc + kd + (ka^2 - 2*ka*kb - \\
& 2*ka*kc + 2*ka*kd \dots \\
& + kb^2 - 2*kb*kc + 2*kb*kd + kc^2 - 2*kc*kd + kd^2)^{(1/2)})) / (ka*kb*(ka^2 \\
& - 2*ka*kb \dots \\
& - 2*ka*kc + 2*ka*kd + kb^2 - 2*kb*kc + 2*kb*kd + kc^2 - 2*kc*kd + \\
& kd^2)^{(1/2)} \dots \\
& + ka*kc*(ka^2 - 2*ka*kb - 2*ka*kc + 2*ka*kd + kb^2 - 2*kb*kc + 2*kb*kd + \\
& kc^2 - 2*kc*kd \dots \\
& + kd^2)^{(1/2)} + kb*kc*(ka^2 - 2*ka*kb - 2*ka*kc + 2*ka*kd + kb^2 - \\
& 2*kb*kc + 2*kb*kd \dots \\
& + kc^2 - 2*kc*kd + kd^2)^{(1/2)} + kc*kd*(ka^2 - 2*ka*kb - 2*ka*kc + \\
& 2*ka*kd + kb^2 - \dots \\
& 2*kb*kc + 2*kb*kd + kc^2 - 2*kc*kd + kd^2)^{(1/2)}); \\
\\
I = & (2*ka*kb) / (ka*kb + ka*kc + kb*kc + kc*kd) + (ka*kb*exp(-(t*(ka + kb + kc + \\
& kd + \dots
\end{aligned}$$

```

(ka^2 - 2*ka*kb - 2*ka*kc + 2*ka*kd + kb^2 - 2*kb*kc + 2*kb*kd + kc^2 -
2*kc*kd + ...
kd^2)^(1/2))/2)*(ka + kb + kc + kd - (ka^2 - 2*ka*kb - 2*ka*kc + 2*ka*kd
+ kb^2 - 2*kb*kc...
+ 2*kb*kd + kc^2 - 2*kc*kd + kd^2)^(1/2)))/(ka*kb*(ka^2 - 2*ka*kb -
2*ka*kc + 2*ka*kd ...
+ kb^2 - 2*kb*kc + 2*kb*kd + kc^2 - 2*kc*kd + kd^2)^(1/2) + ka*kc*(ka^2 -
2*ka*kb - 2*ka*kc...
+ 2*ka*kd + kb^2 - 2*kb*kc + 2*kb*kd + kc^2 - 2*kc*kd + kd^2)^(1/2) +
kb*kc*(ka^2 - 2*ka*kb...
- 2*ka*kc + 2*ka*kd + kb^2 - 2*kb*kc + 2*kb*kd + kc^2 - 2*kc*kd +
kd^2)^(1/2) + kc*kd*(ka^2 ...
- 2*ka*kb - 2*ka*kc + 2*ka*kd + kb^2 - 2*kb*kc + 2*kb*kd + kc^2 - 2*kc*kd +
kd^2)^(1/2)) - (ka*...
kb*exp(-(t*(ka + kb + kc + kd - (ka^2 - 2*ka*kb - 2*ka*kc + 2*ka*kd +
kb^2 - 2*kb*kc + 2*kb*kd + ...
kc^2 - 2*kc*kd + kd^2)^(1/2)))/2)*(ka + kb + kc + kd + (ka^2 - 2*ka*kb -
2*ka*kc + 2*ka*kd + kb^2 ...
- 2*kb*kc + 2*kb*kd + kc^2 - 2*kc*kd + kd^2)^(1/2)))/(ka*kb*(ka^2 - 2*ka*kb -
2*ka*kc + 2*ka*kd + kb^2 ...
- 2*kb*kc + 2*kb*kd + kc^2 - 2*kc*kd + kd^2)^(1/2) + ka*kc*(ka^2 - 2*ka*kb -
2*ka*kc + 2*ka*kd + kb^2 ...
- 2*kb*kc + 2*kb*kd + kc^2 - 2*kc*kd + kd^2)^(1/2) + kb*kc*(ka^2 - 2*ka*kb -
2*ka*kc + 2*ka*kd + kb^2 - ...
2*kb*kc + 2*kb*kd + kc^2 - 2*kc*kd + kd^2)^(1/2) + kc*kd*(ka^2 - 2*ka*kb -
2*ka*kc + 2*ka*kd + kb^2 - 2*kb*kc...
+ 2*kb*kd + kc^2 - 2*kc*kd + kd^2)^(1/2));

```

```

figure
width = 3;      % Width in inches
height = 3;    % Height in inches
alw = 0.75;    % AxesLineWidth
fsz = 11;     % Fontsize
lw = 1.5;     % LineWidth
msz = 8;      % MarkerSize
plot(t,R,'b')
hold on
plot(t,B,'g')
plot(t,I,'r')
set(gca,'XTickLabel',{})
set(gca,'YTickLabel',{})
title('Analytical Solutions')
xlabel('Time')
set(gca,'XTickLabel',{})
set(gca,'YTickLabel',{})
ylabel(['Vesicle/Receptor Complex'])
legend('R(t)', 'B(t)', 'I(t)', 'Location', 'best')

```

```

%%More Complex Numerical Solution%%
% x(1)=R x(2)=B x(3)=I x(4)=C1/a x(5)=C2/b

```

```

% ka=0.0048; %k1
% kb=1.02; %k2
% kc=0.012; %k3
% kd=0.128; %k4%
%Q=32.5;

```

```

Q=3.25;
Qa=Q*.7;
Qb=Q*.3;

%Same Q
f = @(t,x) [kc*x(3)-ka*x(1)*x(5)+kd*x(2);...
    ka*x(5)*x(1)-(kb+kd)*x(2);...
    kb*x(2)-kc*x(3);...
    (x(5)-x(4))*Q;...
    (x(4)-x(5))*Q-ka*x(1)*x(5)+kd*x(2)];

%Varying Q's
f = @(t,x) [kc*x(3)-ka*x(1)*x(5)+kd*x(2);...
    ka*x(5)*x(1)-(kb+kd)*x(2);...
    kb*x(2)-kc*x(3);...
    (Qb*x(5)-Qa*x(4));...
    (x(4)*Qa-x(5)*Qb)-ka*x(1)*x(5)+kd*x(2)];

[t,xa] = ode45(f,[0 7],[2 0 0 5 0],1e-5);%ODE 45 solving for the numerical
solution

figure
width = 3;      % Width in inches
height = 3;    % Height in inches
alw = 0.75;    % AxesLineWidth
fsz = 11;      % Fontsize
lw = 1.5;      % LineWidth
msz = 8;       % MarkerSize
subplot(2,1,1);
plot(t,xa(:,1),'b')
hold on
plot(t,xa(:,2),'g')
plot(t,xa(:,3),'r')
    set(gca,'XTickLabel',{})
    set(gca,'YTickLabel',{})
title('Numerical Solutions')
xlabel('Time')
ylabel('[Vesicle/Receptor Complex]')
legend('R(t)', 'B(t)', 'I(t)')
hold off
subplot(2,1,2);
plot(t,xa(:,4),'m')
hold on
plot(t,xa(:,5),'k')
hold off
set(gca,'XTickLabel',{})
set(gca,'YTickLabel',{})
legend('C1(t)', 'C2(t)', 'Location', 'best')
xlabel('Time')
ylabel('[Vesicles]')

```